

Design of the Deployment Mechanism of Solar Array on a Small Satellite

M. G. El-Sherbiny¹, A. Khattab¹, M.K. Kassab^{2,*}

¹Mechanical Design and Production Eng., Cairo University, Giza, Egypt

²Structure Department, National authority for Remote Sensing & Space Sciences (NARSS), Cairo, Egypt

*Corresponding author: mgsherbiny@yahoo.com

Received December 20, 2012; Revised May 06, 2013; Accepted May 07, 2013

Abstract This paper presents analytical simulation of drag braking during deployment of a solar array system of a small satellite within the space environment, and helps the designer to detect problems during ground testing. The deployment mechanism (DM) is modeled by using Mechanical Desktop (MDT) software and analyzed by using Finite Element Analysis Package (ANSYS 11). Design and Stress analysis of DM is performed at the most critical points during its functioning. Several finite element analysis models were considered to verify the DM integrity. These analyses were correlated with static, modal and random vibration testing. The present work can help in checking the survival of the mechanism under realistic operating conditions and makes sure that it will perform well after an orbit insertion of the satellite.

Keywords: satellite, deployment mechanism, shoe brake, solar Array, finite element, modal analysis

1. Introduction

Today's engineering design needs to manage the conflicting goals, improving performance while reducing developing time and costs. In this context designers utilized the solar energy as clean renewable source for powering small satellites. Solar arrays of considerable surface area are required to provide enough power for the safe payload functioning and for the computer and the communication systems, [1]. Figure 1 shows a schematic drawing of the satellite with the solar arrays [2].

Innovative designs included foldable solar arrays to minimize size and space requirement on the launching vehicle. Self actuated deployment mechanisms utilized the stored energy in a torsion spring to drive the solar arrays during the unfolding phase after orbital insertion. In such cases the motion has to be controlled by drag braking to reduce or eliminate the shock loading at the end of the stroke. Drag brake should be of minimum size and weight but can absorb and dissipate energy enough to make gradual deployment and smooth motion until the mechanism gets to rest at the end of the stroke, without shock loadings or reactions. A special small drum brake, with frictional shoes which are forced in contact with the drum under a compressive spring force, was designed for this particular purpose [3]. Figure 2 shows an isometric drawing of the brake assembly.

The brake has an estimated weight of 0.350Kg and is able to deploy the solar arrays in 2 to 3 seconds depending on the realized coefficient of friction of 0.5 in normal atmosphere and 1.0 in space environment at an altitude of 768Km.

The designed brake has to be checked and tested accurately before the prototype is made available [4].

In the present work the DM is modelled by using Mechanical Desktop (MDT) software and then analyzed by Finite Element Analysis Package (ANSYS 11). Simulation analysis was made to describe the dynamic behavior of the mechanism structure and to predict its natural frequencies and structure response to the worst case of Launch Vehicle (LV) loads through static, modal and random vibration analysis [5].

Mechanical structure can resonate, where small forces can result in significant deformation, and damage can be induced in the structure. Resonant vibration is mainly caused by an interaction between inertial and elastic deformations of the materials within a structure. To better understand structural vibration problems, the resonant frequencies of the structure have to be identified. Modal analysis is recognized as a technique in finding the modes of vibration of machines, and mechanisms [6].

2. Structure and Model Description

The DM is intended for fastening of solar panel to the satellite body, turning the solar panel into the working position and keeping it in this position during operation in orbit. Once the Satellite is in orbit, the Solar Arrays are deployed to function. Therefore, Mathematical Model of DM is constructed and analyzed using finite Element Computer Package (ANSYS 11) to minimize the cost of making prototypes and the time in trial and error practices. Figure 3 shows the MDT model of the designed DM brake assembly to eject the folded SA and to control its deployment under drag braking. The finite element package provides a library of structure elements, such as

beams, shells, and solid elements. The DM is modeled by connecting elements together within the geometrical constraints, taking into consideration material properties,

and appropriate boundary conditions to describe the physical constraints.

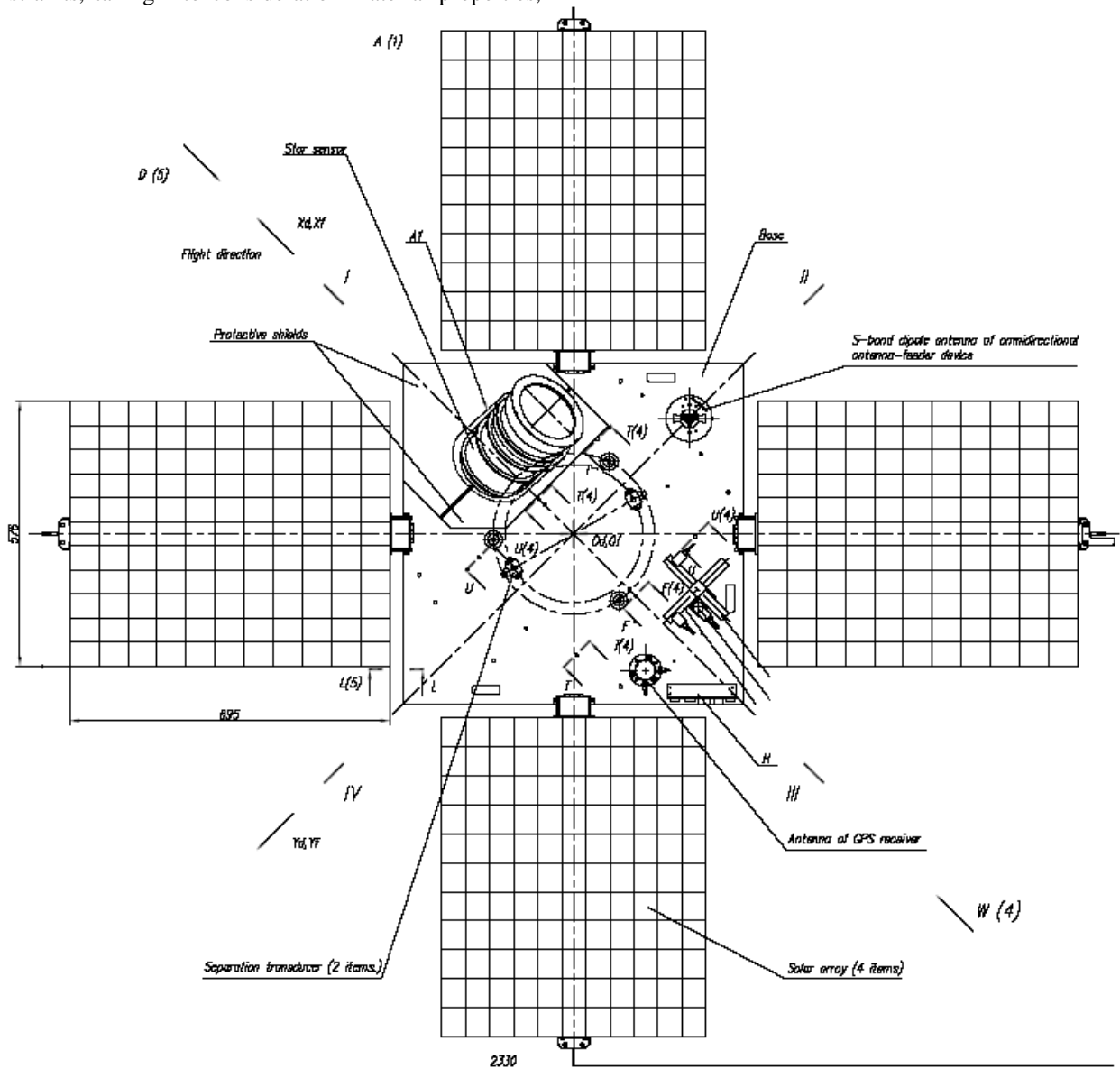


Figure 1. Top view of the satellite with four solar arrays

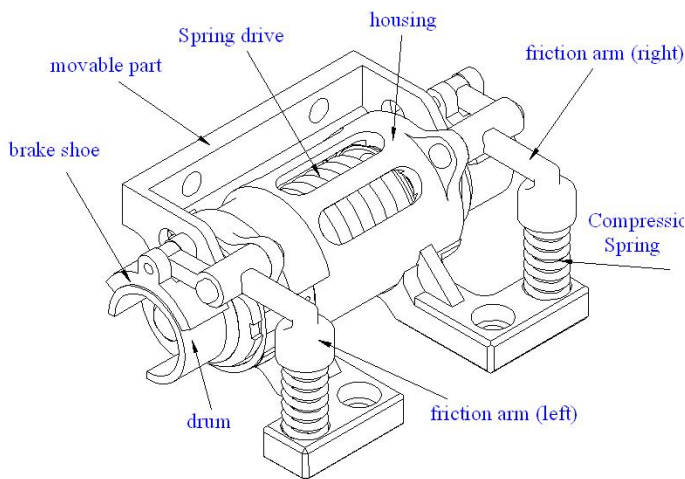


Figure 2. Assembly of shoe brake

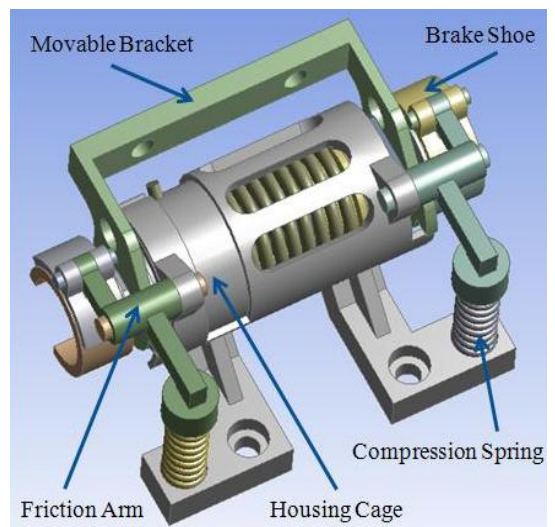


Figure 3. Isometric 3D view of the model

Forces and moments obtained from solar array mechanism and structural analysis are given in [7].

$$F_x = -1.291e-002N, \quad F_y = -5.33e-004 N,$$

$$F_z = -1.651e-002N. \quad M_x = 7.28 e-003N m,$$

$$M_y = -5.795 e-003N m \quad M_z = 5.745 e-003N m.$$

FE analysis of DM is performed to make sure that the DM structure will withstand the loads at the stoppage point. It is recommended to run modal analysis to make sure the natural frequencies of SA will not coincide with the DM ones.

ANSYS 11 FE package is used to make the design analysis and verify the design [8]. The method uses a complex system of points (nodes) which form a grid or a mesh. Fine mesh is used to model fine geometrical details as well as closely approximate the localized stresses and strains in areas of steep gradients or of high stress concentrations. The model represents the assembly of all components and parts of the mechanism linked together and exposed to maximum loading conditions.

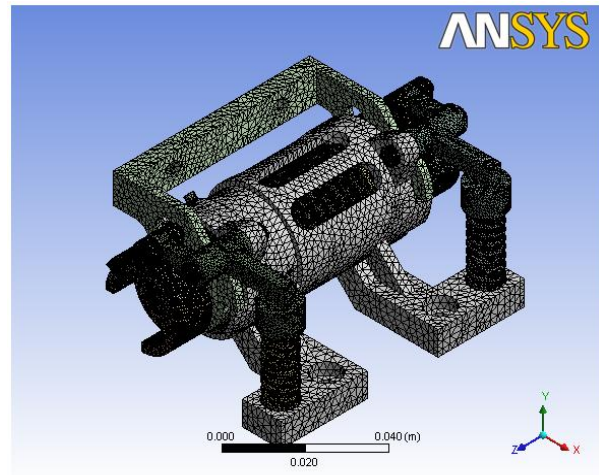


Figure 4. Tetrahedral mesh of the brake mechanism

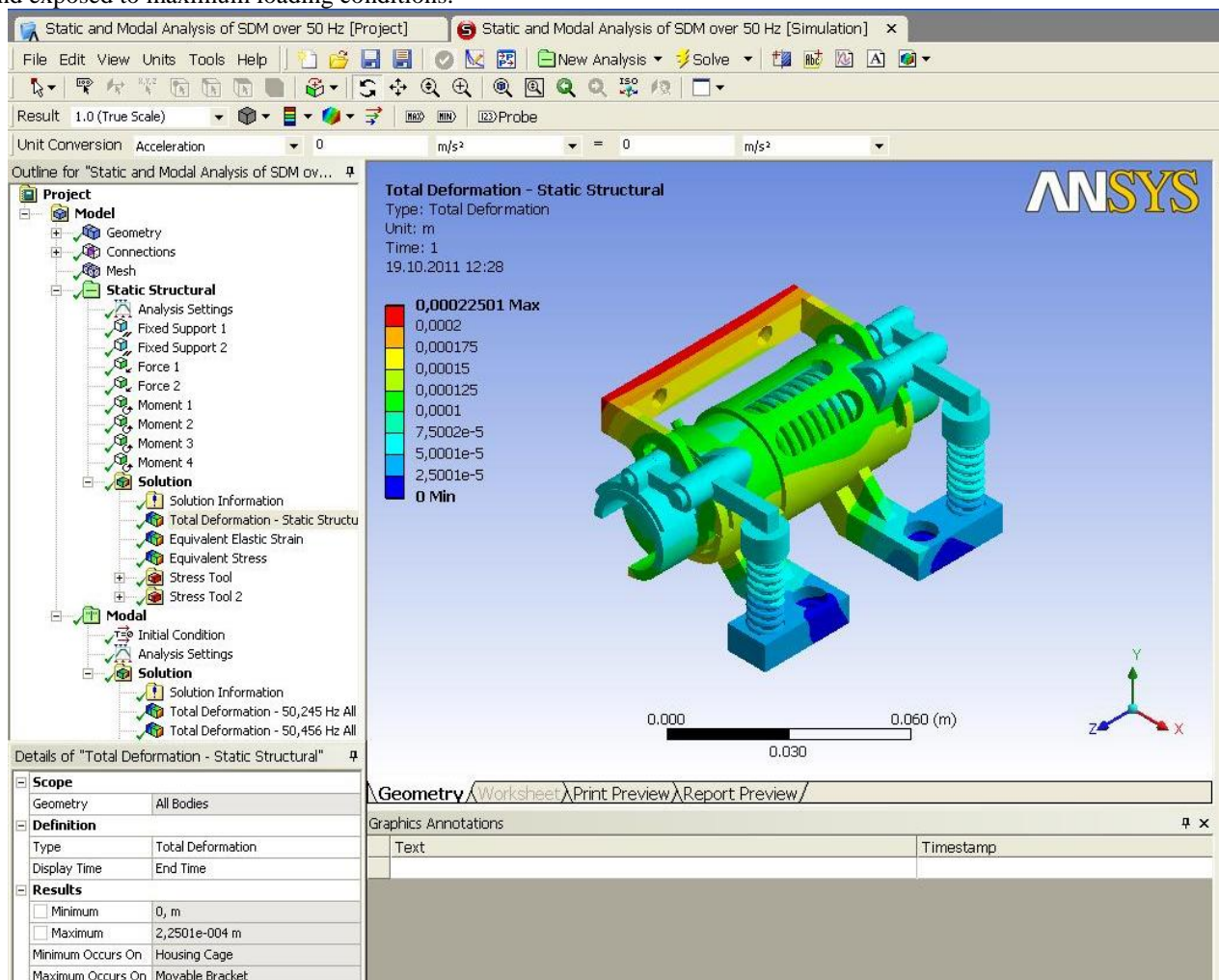


Figure 5. Total Deformation within the mechanism

2. 1. Mesh Generation

Tetrahedral elements are used as shown in Figure 4. When using high relevance of 100, and fine relevance center, the meshing leads to huge sizable number of nodes and elements. But when simplifying relevance to 60 or 50 and selecting a relevance center of medium or coarse, the meshing problem can be smoothly solved.

Using relevance of 100; and relevance center medium, one gets:

No. of elements: 595160;

No. of degrees of freedom (No. of Nodes): 1249356, whilst using relevance of 50; and relevance center medium, gives:

No. of elements was: 90914;

No. of degrees of freedom (No. of Nodes): 194640,

Therefore the later case is more appropriate to minimize truncations and round off errors. Figure 4 shows the mesh design of the DM brake assembly.

2.2. Materials

The materials are selected to meet the requirements of each individual component. Structural steel was selected for parts: rotating shaft, screws, and joints. AISI 4130 steels and 304 stainless steels were used for drums, Gray cast iron is also used for brake shoes, Aluminum alloy AMG6 is used for movable bracket, housing cage and friction arms, whilst other commercial aluminum alloys were used for guiding bushes, and Piano wire spring DIN 17223D is used for spring elements. The mechanical, thermal and physical properties of these materials as employed in the present work are given in appendix I.

3. Static Analysis

The objective of static loading is to define the resulting load distribution, strains and stresses throughout the structure of mechanism components. When performing static analysis under load, static forces and moments are applied to the assembly of the mechanism components. The linear static analysis in ANSYS is used to compute stresses, strains and deformations [9].

Figure 5 represents the ANSYS static analysis from geometry definition passing through connection definition, meshing the model and up to post processing of the static structural results. It also shows the critical areas of the maximum deformation occurs on the movable bracket reaching a maximum computed value as $2,2501e-004$ m. The results indicated that deformations, strains, and stresses are small and did not threaten the structure of SA and the movable bracket.

Figure 6 shows the critical areas of the highest strain in the DM, and also shows the locations of applied loads and the fixed nodal points resembling fixed supports. The analysis showed that the most critical strain occurs on housing cage $2,1718e-002$ m/m.

Figure 7 shows the critical regions or the most stressed regions in the DM. The analysis showed that the most critical stress occurs on cubic joint and its value is $2,7544e+008$ Pa. Obviously the computed max shear stresses were far below the shear strength of the part and therefore the design was mechanically safe under static loading conditions.

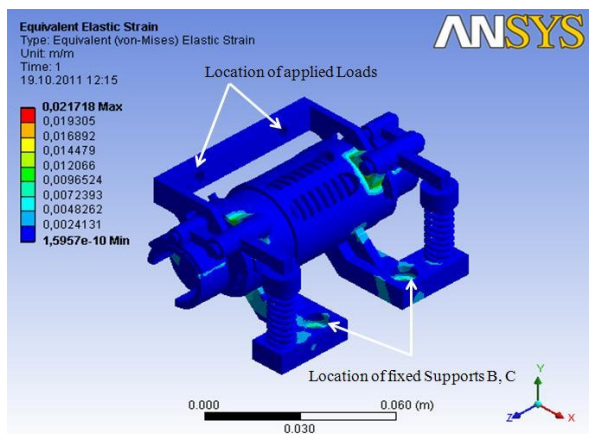


Figure 6. Areas of highly localized strains

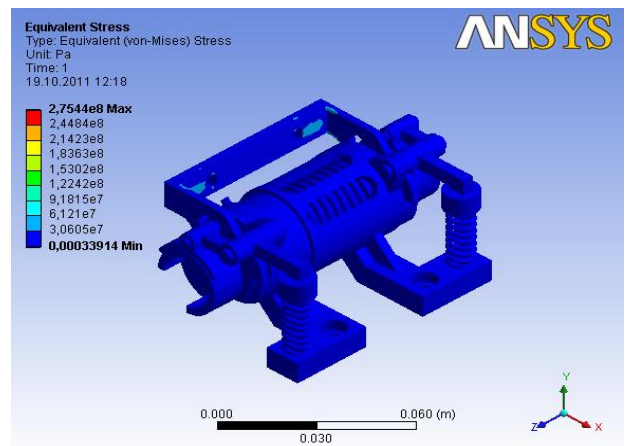


Figure 7. Equivalent Stress distribution (Von-Misses)

4. Modal Analysis of DM

Modal analysis and testing is used to identify the vibration modes and their natural frequencies, and to provide the structural matrices, which is required for the dynamic analysis of the assembly. Thus the basic structural dynamic data, as obtained accurately from a valid test provides a true identification of the structural behavior at the modes of interest. These derived matrices are based on the measured contributions of the mass, stiffness and damping properties at the modes of interest, taking into considerations the actual boundary conditions. These data is introduced into a finite element model of the structure, for subsequent problem solving, or re-designing the mechanism for better dynamic response [9].

Modal analysis was performed to the model of DM using ANSYS 11 software and the model has been solved for the first 5 modes. Figure 8 and Figure 9 show the resulting first two modes of vibration. This analysis is also used to gain better understanding of DM behavior and response to environmental conditions which of course, lead to better planning of the experimental testing.

The normal modes obtained from the FEA for DM model before testing, represent fairly reasonable estimation of the DM Eigen frequencies and mode shapes. This information is used to plan the real testing; that is, to determine excitation conditions, shaker locations and accelerometer locations.

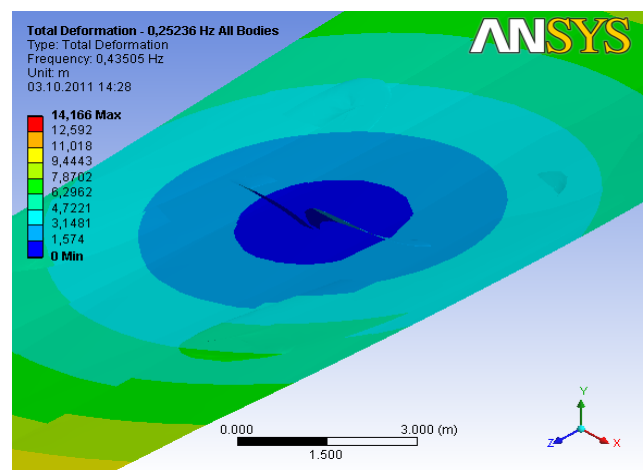


Figure 8. First mode shape of DM structure at $f_n = 0.25236$ Hz

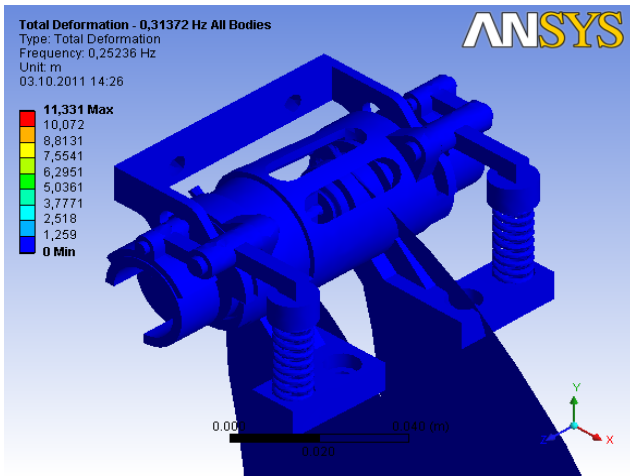


Figure 9. Second mode shape of DM structure at $f_n = 0.31372$ Hz

5. Random Analysis

The fundamental nature of random vibration are needed to verify design, develop and produce cost effective and lightweight mechanisms that are capable of operating in various environments with high degree of reliability. The characteristic of random vibration is non-periodic and it can be considered as a series of overlapping sinusoidal curves [9,10,11]. In this environment all the exciting frequencies within a given bandwidth are excited at the same time.

One of the different types of curves that can be used to show the random vibration input requirements is the Power Spectral Density (PSD) curve. Table (1) shows the PSD data. This is also shown in log-log scale with power spectral density (G^2/Hz) along the ordinate vertical axis and frequency (Hz) along the horizontal abscissa axis. It should be noted that acceleration is represented as root mean square (RMS) and it is the area under the random vibration curve. Figure 10 shows the shaped random vibration input curve for the DM model.

Table (1). PSD Acceleration vs. Frequency

Frequency Hz	PSD Acceleration (m/sec ² /Hz)
10,0	1,0
25,0	1,3
50,0	1,0
80,0	3,1
130,0	1,6
160,0	2,8
190,0	1,2
225,0	2,0
270,0	2,8
310,0	5,0

Figure 11 shows the resulting stresses of DM analysis and it is seen that stress distribution values have occurred at scale factor 1 sigma, and probability of 68.3% of the time at X-axis direction. It also, shows that the maximum effect of frequencies occurs on Torsion Spring and

compression spring with a value of 733.18Pa. These stresses are far below the material failure limits, do not form threatening for DM, and implies that DM can withstand vibration loads well after an orbit insertion of the satellite.

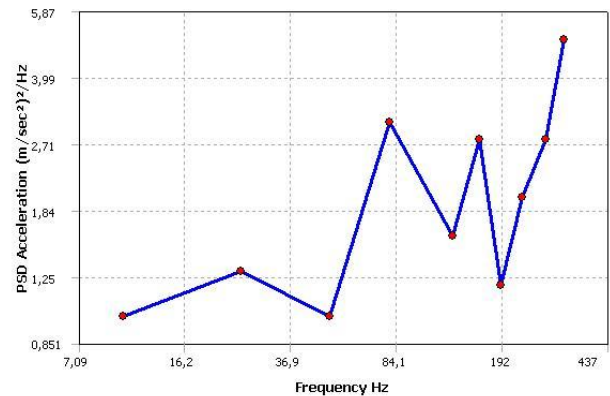


Figure 10. PSD Acceleration versus Frequency

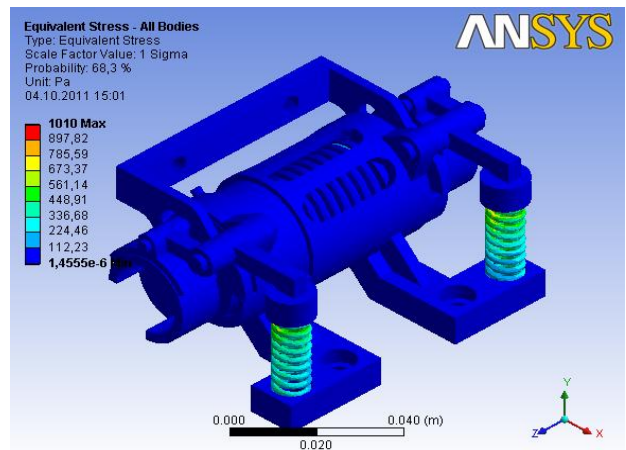


Figure 11. Stress distribution on the DM model

Deformations occurred under the effect of frequencies load at all directions (X, Y, and Z) and the resulting deformations due to velocity and acceleration loads did not represent a threat to any of the DM components.

Figure 12, Figure 13 and Figure 14 show the deformation due to directional displacement, velocity and acceleration along the X axis.

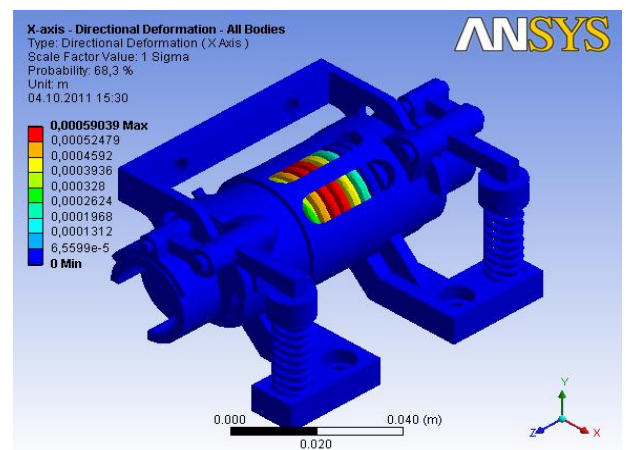


Figure 12. Deformation due to displacement of DM mechanism on X axis

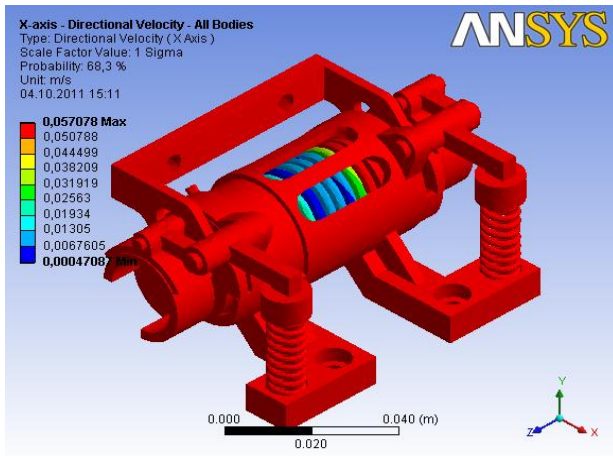


Figure 13. Deformation due to velocity on X axis

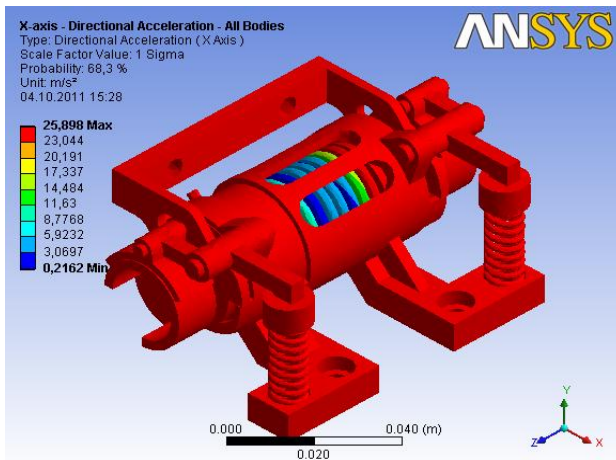


Figure 14. Deformation due to acceleration on the X axis

6. Conclusion

Linear static analysis of the DM is performed using FE analysis on ANSYS software and the deformation and displacement are computed. The modal analysis was conducted and the first five resonance frequencies (mode shapes) are calculated. Results obtained from Random vibration analysis revealed that the maximum stresses occurred on Torsion Spring and Compression Spring with a value of 733.18Pa. The FE analysis of the proposed design of the DM for SA of a small satellite showed that the model survived vibration loads, moments, and forces at operating conditions similar to those expected after an orbit insertion of the satellite. The present work also shows that the designed small shoe brake can be used to control the unfolding and protect the solar panels from shock loads and damage at the end of the deployment.

References

[1] Heylen W., Lammens S., Sas P.: *Modal Analysis Theory and Testing*, Katholieke Universiteit, Leuven, 1997.
 [2] Egypt Sat-1 Project, *Satellite Preliminary Design*. Album of Drawings. Doc. No. EGS YZH RPT 01801, NARS, EGYPT, 2007.
 [3] Kassab, M. “*Design, Analysis, Manufacturing, and Testing of a Deployment Mechanism for Solar Panel of a Small Satellite*”; Ph.D. thesis, Faculty of Engineering, Cairo University, Egypt, December 2011.

[4] Friswell, M. I., Mottershead J. E., “*Finite Element Model Updating in Structural Dynamics*” Dept. of Mechanical Engineering, University of Swansea, Swansea, U.K. Springer, Solid Mechanics and Its Applications, Vol. 38, P292. 1996.
 [5] Shibabrat N., Wrik M., “*Experimental Modal Testing for Estimating the Dynamic Properties of a Cantilever Beam*”, Department of Civil Engineering, Jadavpur University, Kolkata-700 032. <http://fostonlietne.org/Thought/CA-77.pdf>.
 [6] Bart B. Wim H. and Jan D.; “*Modern Solutions for Ground Vibration Testing of Large Aircraft*”; LMS International, Leuven, Belgium, SAE International Journal of Aerospace, April, 2009, Vol. 1, No. 1, pp. 732-742, 2009.
 [7] EgyptSat-1 Project, *Satellite Preliminary Design. Composition and main Characteristics*, Doc. No. EGS YZH RPT 01400 issue 2. 2007.
 [8] ANSYS, Inc. Release 11.0 Documentation for ANSYS.
 [9] Sudharsan, M; “*Structural Design and Analysis of a lightweight Composite Sandwich Space Radiator Panel*” Msc. Thesis, Office of Graduate Studies of Texas A&M University, USA, December 2003.
 [10] Neville F. Rieger; “*the Relation between Finite Element Analysis and Modal Analysis*”; Stress Technology Incorporated, Rochester, New York. 2008.
 [11] Fufa, B.; Zaho, C.; and Wensheag, M.; “*Modeling and Simulation of Satellite Solar Panel Deployment and Locking*” Information Technology Journal 9 (3): pp. 600-604, 2010.

Appendix I

Table 1. Properties of Structural Steel

Structural	
Young's Modulus	2,e+011 Pa
Poisson's Ratio	0,3
Density	7850, kg/m ³
Tensile Yield Strength	2,5e+008 Pa
Tensile Ultimate Strength	4,6e+008 Pa
Thermal	
Thermal Conductivity	60,5 W/m ·°C
Specific Heat	434, J/kg ·°C

Table 2. Properties of Aluminum Alloy

Structural	
Young's Modulus	7,1e+010 Pa
Poisson's Ratio	0,33
Density	2770, kg/m ³
Tensile Yield Strength	2,8e+008 Pa
Tensile Ultimate Strength	3,1e+008 Pa
Thermal	
Specific Heat	875, J/kg ·°C

Table 3. Properties of Steel Standard AISI 4130

Structural	
Young's Modulus	2,e+005 Pa
Poisson's Ratio	0,3
Density	7700, kg/m ³

Table 4. Properties of Stainless Steel 316

Structural	
Young's Modulus	1,93e+011 Pa
Poisson's Ratio	0,31
Density	7750,kg/m ³
Tensile Yield Strength	2,07e+008 Pa
Tensile Ultimate Strength	5,86e+008 Pa
Thermal	
Thermal Conductivity	15,1W/m °C
Specific Heat	480,J/kg ·°C

Table 5. Properties of Aluminum Alloy AMG6

Structural	
Young's Modulus	7,1e+010 Pa
Poisson's Ratio	0,33
Density	2770,kg/m ³
Thermal	
Specific Heat	875,J/kg ·°C

Table 6. Properties of Piano Wire Steel DIN 17223D

Structural	
Young's Modulus	2,06e+011Pa
Poisson's Ratio	0,29
Density	7850,kg/m ³
Thermal	
Specific Heat	450,J/kg ·°C

Table 7. Properties of Gray Cast Iron

Structural	
Young's Modulus	1,1e+011Pa
Poisson's Ratio	0,28
Density	7200,kg/m ³
Tensile Ultimate Strength	2,4e+008Pa
Thermal	
Thermal Conductivity	52,W/m ·°C
Specific Heat	447,J/kg ·°C